When May a Nonuniform Distribution of ^{131}I Be Considered Uniform? An Experimental Basis for Multicellular Dosimetry

Prasad V.S.V. Neti, PhD; and Roger W. Howell, PhD

Division of Radiation Research, Department of Radiology, New Jersey Medical School, University of Medicine and Dentistry of New Jersey, Newark, New Jersey

To varying degrees, radiopharmaceuticals are distributed nonuniformly in tissue. At a macroscopic level, the radiopharmaceutical may appear to be uniformly distributed throughout the tissue. However, on closer inspection, not all cells in the tissue may be labeled with the radiopharmaceutical. Furthermore, the radioactivity in the cells may be localized only in certain compartments within the cell. This work uses a cell culture model to examine the impact of nonuniformities at the multicellular level on the lethal effects of ^{131}I. **Methods:** A 3-dimensional tissue culture model was used to investigate the biologic effects of nonuniform distributions of ^{131}I in a large population of mammalian cells. Chinese hamster V79 cells were labeled with ^{131}I-iododeoxyuridine (^{131}IdU), mixed with unlabeled cells, and multicellular clusters (4×10^6 cells) were formed by gentle centrifugation. Thus, the labeled cells were randomly located in the cluster to achieve a uniform distribution of radioactivity at the macroscopic level, yet nonuniform at the multicellular level. The clusters were assembled as described and then maintained at 10.5°C for 72 h to allow ^{131}I decays to accumulate. The clusters were then dismantled and the cells were plated for colony formation. **Results:** When 100% of the cells were labeled, the surviving fraction of cells in the cluster was exponentially dependent on the cluster activity down to 0.1% survival. In contrast, when 10% of the cells were labeled, it was observed that the survival fraction begins to saturate at about 1% survival. Absorbed-dose estimates reveal that the mean lethal cluster dose is 4.5, 5.7, and 6.4 Gy for 100%, 10%, and 1% labeling, respectively. **Conclusion:** These data indicate that when the distribution of ^{131}I is uniform at the macroscopic level, but nonuniform at the multicellular level, the mean absorbed dose to a tissue element may not be a suitable quantity for use in predicting biologic effect. Rather, cellular and multicellular dosimetry approaches may be necessary to predict the biologic effects of incorporated ^{131}I.

Key Words: ^{131}I; iododeoxyuridine; dosimetry; multicellular cluster; V79 cells; survival

J Nucl Med 2003; 44:2019–2026

Received Apr. 30, 2003; revision accepted Sep. 8, 2003.

For correspondence contact: Roger W. Howell, PhD, Department of Radiology, MSB F-451, New Jersey Medical School, UMDNJ, 185 S. Orange Ave., Newark, NJ 07103.

E-mail: rhowell@umdnj.edu

Radionuclides that undergo β-decay are widely used in biomedical research and in medical procedures. Furthermore, they are often encountered in environmental accidents such as the Chernobyl incident. The β-emitter ^{131}I is perhaps one of the most widely recognized radionuclides in this category because of its carcinogenic hazard to the thyroid in the case of accidental exposures and its potent therapeutic efficacy against thyroid cancer when used in the form Na^{131}I. The mean energy of the principal β-particles emitted by ^{131}I is 191 keV (*1*) with a corresponding mean range in water of about 400 μm (*2*). Therefore, when this radionuclide is localized within a cell, the β-particles emitted typically irradiate target cells about 30–40 cell diameters distant. Accordingly, the impact of the limited range of the ^{131}I β-particles has stirred considerable debate regarding the biologic consequences of nonuniform distributions of this radionuclide in tissue.

Early discussions on the dosimetric and biologic implications of nonuniform distributions of ^{131}I began soon after its introduction to medicine (*3–5*). Issues concerning nonuniform distributions of β-emitters continue to be of considerable interest and debate even at present (*6,7*). Over the years, numerous theoretical models have been developed to explore the dosimetric implications of nonuniform distributions of ^{131}I both from the standpoint of radiation protection as well as radiation therapy (*8–18*). The experimental basis for such theoretical calculations has largely been autoradiographic data (*3,4,19–21*). Recent calculations have melded nonuniform dose distributions with dose–response modeling to arrive at predictions of biologic responses to nonuniform distributions of ^{131}I (*22*).

Although there has been extensive theoretical modeling of the dosimetry and biologic response to nonuniform distributions of ^{131}I, little of this modeling was based on measurements of biologic responses to distributions of ^{131}I where the nonuniform distribution of the radionuclide was controlled and known with precision (*7*). Kwok et al. (*23*) and Langmuir et al. (*24*) used multicellular spheroids to investigate the effects of ^{131}I-labeled monoclonal antibodies. However, the spheroid model largely restricted the radioac-

tivity to the periphery of the cluster, thus making it possible to only study the effects of a spherical shell distribution. In this work, the lethal effects of nonuniform distributions of ^{131}I are studied using an in vitro multicellular cluster model wherein the variables affecting distribution of radioactivity can be tightly controlled. This has been accomplished by assembling multicellular clusters containing 4×10^6 cells wherein 1%, 10%, or 100% of the cells are radiolabeled. This tight control over the distribution of radioactivity allows one to maintain what appears to be a uniform distribution at a macroscopic level, while altering the nonuniform distribution at the multicellular level. This permits a well-controlled investigation of the biologic consequences of nonuniform activity distributions of ^{131}I at the multicellular level.

TABLE 1
Parameters Used in Preparation of Multicellular Clusters

Cells labeled with ^{131}IdU (%)	Activity concentrations used for cell labeling (kBq/mL)	Incorporated radioactivity per labeled cell (mBq/cell)	No. of cells in cluster*	
			Unlabeled	Labeled
100	0–150	0–16	0	4.0×10^6
10	0–550	0–300	3.6×10^6	4.0×10^5
1	0–1,200	0–750	3.96×10^6	4.0×10^4

*Coulter counter is used to determine cell concentrations that are in turn used to prepare clusters. Statistical accuracy of Coulter counter is about 5%. Accordingly, statistical uncertainty in number of cells in cluster is also about 5%.

MATERIALS AND METHODS

Radiochemical and Quantification of Radioactivity

^{131}I as Na^{131}I was obtained from Perkin Elmer Life Sciences in 0.1N NaOH (13.6 GBq/mL). Radiolabeled iododeoxyuridine (^{131}IdU) was synthesized and purified by high-performance liquid chromatography in our laboratory according to procedures previously reported (*25*). The ^{131}I activity was quantified with a Canberra HpGe well detector (364.5-keV photopeak, photopeak efficiency = 0.33, yield = 0.812) or a Packard automatic γ-counter equipped with a 3 in. (7.62 cm) sodium iodide well crystal (overall efficiency = 0.78 in the energy window 260–470 keV). The radionuclide ^{131}I undergoes β-decay with a physical half-life of 8.04 d.

Cell Line

Chinese hamster V79 lung fibroblasts were used in this study, with clonogenic survival serving as the biologic endpoint. The different minimum essential media (MEMA, MEMB, and wash MEMA) and culturing conditions were described in detail in a previous publication (*26*). The plating efficiency was typically about 60%. All media and supplements used in this study were from Life Technologies. Cells were maintained in Falcon (Becton Dickinson) 225-cm^2 sterile tissue culture flasks at 37°C in a humidified atmosphere with 95% air/5% CO_2 and subcultured twice weekly or as required on reaching 80%–90% confluence. The cell line was tested to be free of mycoplasma.

Assembly of Multicellular Clusters

Multicellular clusters containing nonuniform distributions of ^{131}I were assembled according to protocols described in detail elsewhere (*26–28*). Briefly, V79 cells growing as monolayers in 225-cm^2 Falcon flasks were washed with 20 mL of phosphate-buffered saline, trypsinized with 0.05% trypsin and 0.53 mmol/L ethylenediaminetetraacetic acid, and suspended at 4×10^5 or 4×10^6 cells per milliliter in calcium-free MEM with 10% heat-inactivated (57°C, 30 min) fetal calf serum, 2 mmol/L L-glutamine, 50 units/mL penicillin, and 50 μg/mL streptomycin (MEMB). Aliquots of 1 mL were placed in 2 sets of sterile 17 × 100 mm Falcon polypropylene round-bottom culture tubes (10 tubes in each set) and placed on a rocker-roller (Fisher Scientific) for 3–4 h at 37°C in an atmosphere of 95% air/5% CO_2. After this conditioning period, 1 mL of MEMB containing various activities of ^{131}IdU was added to 1 set of tubes (denoted "labeled;" range of concentrations in Table 1). To the second set of tubes, 1 mL of MEMB was added (denoted "unlabeled"). The tubes were returned to a rocker-roller at 37°C, 95% air/5% CO_2. After 14 h, the cells were washed 3 times with 10 mL of wash MEMA, resuspended in 5 mL of MEMA, and passed 5 times through a 21-gauge needle. The cell concentration in each tube was determined with a calibrated Coulter model ZM cell counter (Coulter Electronics), then mixed with unlabeled cells to get 100%, 10%, or 1% radiolabeled cells in a total population of 4×10^6 cells (Table 1), and centrifuged at 2,000 rpm, 4°C for 10 min. The supernatant was decanted, the pellets were disrupted, and the entire ~200 μL of this final cell suspension was transferred directly to a sterile 400-μL polypropylene microcentrifuge tube (Helena Plastics). The tube was washed with an additional 200 μL of MEMA and the wash was transferred to the same 400-μL polypropylene microcentrifuge tube. The 400-μL tubes were then centrifuged at 1,000 rpm for 5 min at 4°C to form clusters (4×10^6 cells; Fig. 1). The capped microcentrifuge tubes containing the clusters were placed in a perforated microcentrifuge tube rack and maintained in a refrigerator at 10.5°C. This temperature was selected because V79 cells can remain in the cluster configuration at this temperature for long periods of time (up to 72 h) without decrease in plating efficiency. This was also true for V79 cells in suspension culture (*26*). Therefore, the cells accumulate the preponderance of their radioactive decays while in the cluster configuration as opposed to the radiolabeling and colony-forming periods.

Determination of Surviving Fraction of Cells in Multicellular Clusters

After 72 h at 10.5°C, the supernatant was carefully removed and the tube was vortexed to disperse the cell cluster. The cells were resuspended in MEMA, transferred to 17 × 100 mm Falcon polypropylene tubes, washed 3 times with 10 mL of wash MEMA, resuspended in 2 mL of MEMA, passed through a 21-gauge needle 5 times to disperse cells, and serially diluted in wash MEMA (four 10× dilutions), and 1 mL of the appropriate dilutions (approximately 200 cells for control tubes) were seeded in triplicate into 60 × 15 mm Falcon tissue culture dishes containing 4 mL of MEMA. The dishes were then placed in an incubator at 37°C with 95% air/5% CO_2. Aliquots were taken from each tube before serial dilution and the mean radioactivity per labeled cell was determined (Table 1). The tissue culture dishes were removed from the incubator after 1 wk and the resulting colonies were washed 3 times with normal saline, washed 2 times with ethanol to fix, and finally

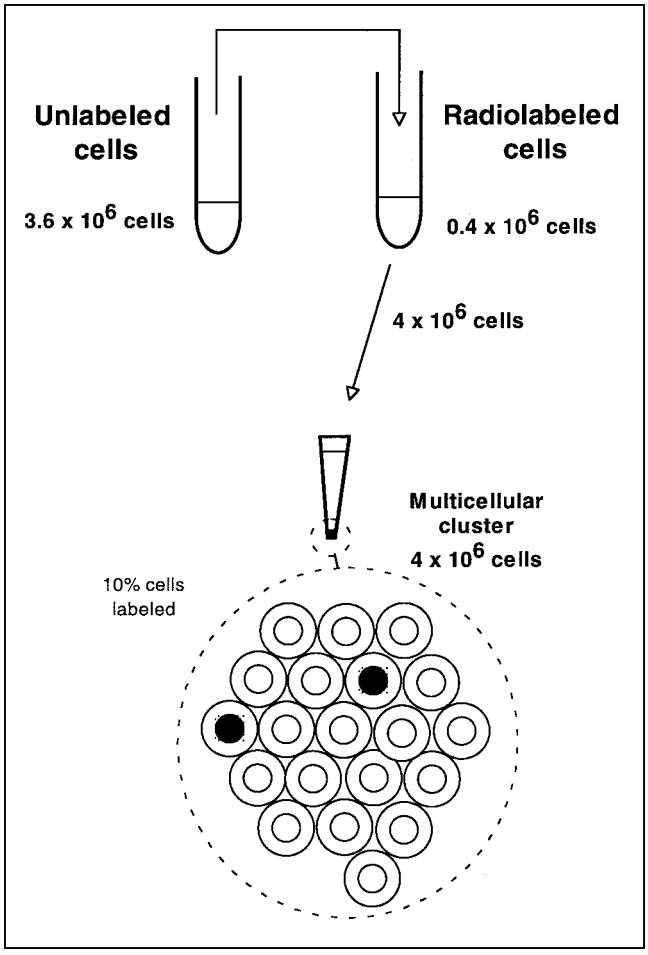

FIGURE 1. Assembly of multicellular cluster of V79 cells wherein 10% cells were radiolabeled with ^{131}IdU.

stained with 0.05% crystal violet. The numbers of colonies were counted with a dissecting microscope at 40× magnification. A colony count of 25–250 was considered as a valid data point for each tissue culture dish. The surviving fraction compared with parallel control was determined for each radioactivity concentration used.

Response of Multicellular Clusters to Chronic External γ-Rays

Irradiation of multicellular clusters with ^{137}Cs γ-rays allows determination of the response of the cell population to a uniform dose of low-LET ionizing radiation. The response of the clusters to chronic external γ-rays was initially assessed in our earlier study (*26*). However, in that study, the lowest survival fraction achieved was only about 50% due to technical limitations of the ^{137}Cs source used to irradiate the samples. This did not allow us to observe the shape of the survival curves at lower survival fractions, an important region of the curve for comparison with the survival curves for ^{131}IdU. Accordingly, a styrofoam box containing a coil of Tygon tubing lining the inside walls was placed inside a JL Shepherd Mark I ^{137}Cs irradiator (with 200× Pb attenuators) and the ends of the tubing were fed through the pass-throughs on the side of the irradiator. Cooled water was continuously circulated through the tubing using a Neslab model 115 circulator equipped with a temperature feedback probe to maintain the inside of the box at precisely 10.5°C. Once equilibrium temperature was reached, microcentrifuge tubes containing multicellular clusters prepared with 4×10^6 unlabeled cells as described above were placed in the box at different distances from the 222-TBq (6,000 Ci) ^{137}Cs source. Two control tubes were similarly maintained at 10.5°C without radiation exposure. The cumulated absorbed dose to each tube was measured using a Thomson-Nielson miniature MOSFET dosimeter system. After 72 h of chronic irradiation, the cells were processed as described above to determine the cell survival fraction. Cumulated doses ranging from 2.4 to 52 Gy were delivered over 72 h at dose rates from about 3 to 80 cGy/h, depending on the distance from the source. After the chronic irradiation, the cells were processed as above and the survival fraction was determined compared with that of unirradiated control cells.

Measurement of Cluster Mass

Our previous studies focused on ^{3}H and ^{125}I localized in the cell nucleus. These radionuclides emit very short-range radiations and therefore cellular dosimetry was most relevant. However, in the case of ^{131}I, where the mean range of the β-particles is about 400 μm, the mean absorbed dose to the cluster is of interest. Accordingly, the cluster mass was determined to facilitate the absorbed-dose calculation. This was done carrying out all preparations described above for 10 clusters of 4×10^6 cells; however, before assembling the clusters, the cells were pooled into a single sterile 17 × 100 mm Falcon polypropylene round-bottom culture tube. The resulting 40×10^6 cells were transferred to the standard 400-μL microcentrifuge tube for making clusters and the tube was then gently centrifuged at 1,000 rpm for 5 min. The resulting pellet of 40×10^6 cells was then placed in an incubator at 10.5°C. After 72 h, the supernatant was carefully aspirated using a Pasteur pipet (stretched under heat to form a small bore opening) and the tube was weighed on an electronic balance (±0.1 mg). The cluster was then removed by aspiration and the tube reweighed. The cluster weight was the difference between the 2 measurements. Two clusters of 40×10^6 cells were analyzed in separate experiments with the average weight being 79 ± 1 mg. Therefore, the average cluster weight for 4×10^6 cells was 7.9 ± 0.1 mg. This approach was originally attempted to directly determine the mass of a 4×10^6 cell cluster; however, the inaccuracies associated with aspiration of the supernatant from above the small cluster and evaporation during transport to the electronic balance interfered with the accuracy of the measurements. To ensure the accuracy of the pooled approach, the weights of additional clusters of 10×10^6, 20×10^6, and 30×10^6 were also determined. In these cases, the average weights per 4×10^6 cells were 7.910, 7.960, and 7.926 mg, respectively. Therefore, these measurements also yielded the same result as the 40×10^6 cell cluster, thereby reflecting the precision of this approach.

RESULTS

Uptake of ^{131}IdU in V79 Cells

Previous results have shown that the uptake of ^{131}IdU (and ^{125}IdU) is linear in time over the 14-h incubation period on the rocker-roller at 37°C (*29*,*30*). In addition, uptake of ^{131}IdU (and ^{125}IdU) is also linearly dependent on the concentration of ^{131}IdU in the culture medium (*29*,*30*). This was observed in the present studies as well as shown in Figure 2. It may be observed that the slope of the 100% labeling case is lower (~0.1 mBq per cell per kBq/mL) than that in the

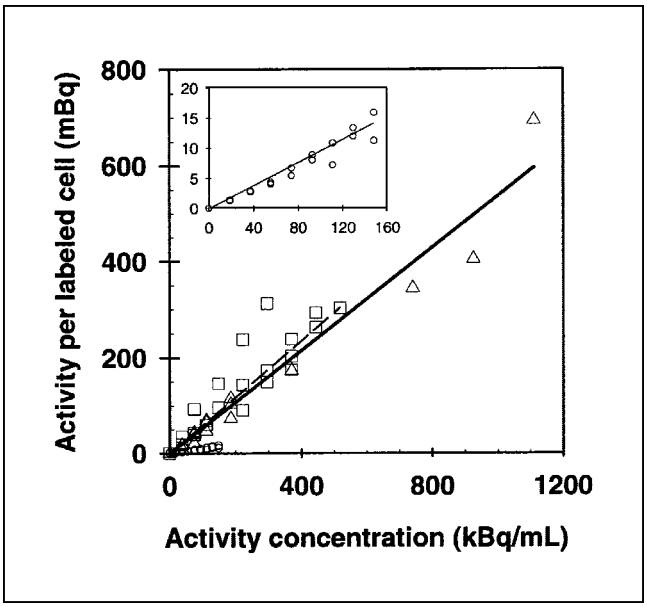

FIGURE 2. Dependence of cellular uptake of ^{131}I on initial extracellular concentration of ^{131}IdU in culture medium. Different symbols correspond to data collected during experiments involving 100% (○), 10% (□), or 1% (△) labeling. In 100% case, 4×10^6 cells were labeled, whereas 4×10^5 cells were labeled to prepare 10% and 1% (only 4×10^4 cells were used) cases. Linear least-squares fit of data is also shown for each case: 100% (thin line), 10% (dashed line), 1% (bold line). Inset shows enlargement of 100% case.

10% and 1% cases (~0.6 mBq per cell per kBq/mL). This may be due to the fact that 4×10^5 cells were labeled for preparation of the 10% and 1% clusters, whereas 4×10^6 cells were labeled for the 100% cluster.

Response of Multicellular Clusters to ^{131}IdU

Figure 3 shows the surviving fraction of cells in the multicellular cluster as a function of the ^{131}I activity in the cluster when 100%, 10%, or 1% of the cells were radiolabeled. The response curve for 100% labeling is exponential over a range of 3 logarithms of kill, whereas the curve for 10% labeling appears as a 2-component exponential over the same range. Due to limitations regarding preparation of ^{131}IdU and loading of cells with high activities, it was only possible to observe survival fractions down to about 0.05 when only 1% of the cells were labeled. The data for each labeling condition were least-squares fit to a 2-component exponential function:

$$SF = (1 - b)e^{-A/A_1} + be^{-A/A_2} \qquad \text{Eq. 1}$$

where SF is the survival fraction, A is the cluster activity, and b, A_1, and A_2 are the fitted parameters. For 10% labeling, the fitted parameters b, A_1, and A_2, are 0.00777 ± 0.00109, 21.7 ± 2.5 mBq per labeled cell, and 370 ± 333 mBq per labeled cell, respectively. In the case of 100% and 1% labeling, with $b = 0$, the fitted values of A_1 are 1.71 ± 0.039 and 241 ± 12.6 mBq per labeled cell, respectively. The fitted parameters are summarized in Table 2.

For the medium energy β-emitter ^{131}I where cross-irradiation plays a major role in the absorbed dose to the labeled and unlabeled cells, it is instructive to plot the survival fraction as a function of cluster activity (Fig. 4). These data are also least-squares fit to Equation 1, and the resulting fitted parameters are summarized in Table 2.

Response of Multicellular Clusters to External γ-Rays

Figure 5 shows the dose–response curves for multicellular clusters of V79 cells exposed to chronic ^{137}Cs γ-rays delivered over a 72-h period. The historical response to ^{137}Cs γ-rays is also shown for comparison (*26*). A least-squares fit of these data to the linear-quadratic model ($SF = \exp(-\alpha D - \beta D^2)$) yielded $\alpha = 0.0487 \pm 0.022$ Gy^{-1}, $\beta = 0.00267 \pm 0.00040$ Gy^{-2}. Interestingly, these values are very close to our previously reported values that were based on a fit to data corresponding to the triangles in Figure 5 that have a maximum kill of only about 50% (*26*). Based on these parameters, the absorbed dose of chronic ^{137}Cs γ-rays that is required to achieve 37% survival D_{37} is 12.2 ± 2.4 Gy.

DISCUSSION

Radioiodinated pharmaceuticals are widely used in clinical medicine to diagnose and treat a variety of medical conditions. It is well known that these radiopharmaceuticals localize in different tissues in the body and that their distribution at the macroscopic and microscopic levels is nonuniform. The degree of nonuniformity can have a profound

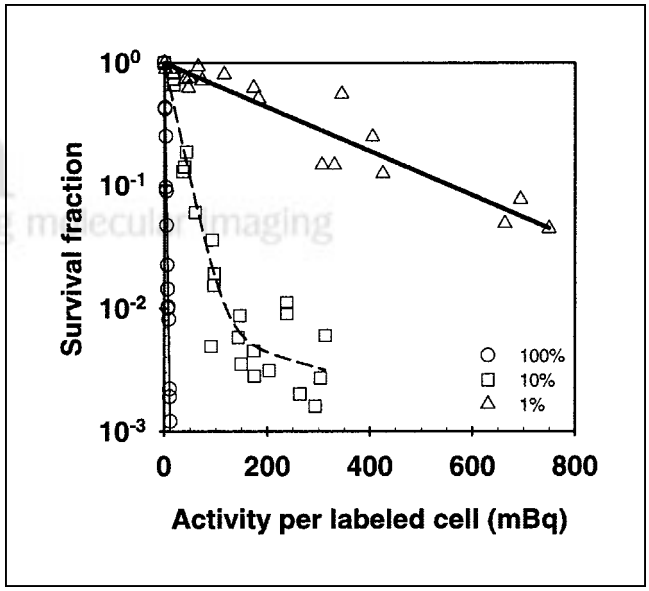

FIGURE 3. Survival of V79 cells in multicellular clusters as function of initial ^{131}I activity per labeled cell. Data are shown for experiments where 100% (○), 10% (□), or 1% (△) of cells in multicellular cluster were labeled with ^{131}IdU. Clusters were maintained at 10.5°C for 72 h and then survival fraction was determined compared with that of cells from control clusters (0% labeled). Data from 3 independent experiments are plotted for each labeling condition. Least-squares fits of data are shown for each labeling condition.

TABLE 2
Fitted Parameters for Multicellular Cluster Survival Curves

Treatment	Cells labeled (%)	$b^{*\dagger}$	A_1^* (mBq/cell)	A_2^* (mBq/cell)	$A_1^\dagger$ (kBq/cluster)	$A_2^\dagger$ (kBq/cluster)
^{131}IdU	100	0	1.71 ± 0.039	—	6.84 ± 0.16	—
^{131}IdU	10	0.00777 ± 0.00109	21.7 ± 2.5	370 ± 333	8.68 ± 1.00	148 ± 133
^{131}IdU	1	‡	241 ± 12.6	‡	9.64 ± 0.50	‡

*Least-squares fit to data in Figure 3.
†Least-squares fit to data in Figure 4.
‡Unknown; insufficient data in this region.
Values of fitted parameters are based on least-squares fits to $SF = (1 - b)e^{-A/A_1} + be^{-A/A_2}$. SEs are indicated.

impact on the biologic response to the radiopharmaceutical. Despite these well-known facts, current internationally accepted methods for assessing risks from diagnostic nuclear medicine procedures assume that the radioactivity in organs and tissues is uniformly distributed and that the biologic response depends principally on absorbed dose, radiation type, and tissue radiosensitivity (*31*). Several investigators have raised important concerns regarding the assumption of uniform distribution of radioactivity and their impact on risk estimates and therapeutic response (*6*,*22*,*32*). However, one of the major stumbling blocks to predict the biologic response of tissues with nonuniform distributions of radioactivity has been the absence of experimental models that allow tight control over the distribution of the radioactivity (*7*). The present data for ^{131}I were obtained with a 3-dimensional tissue culture model that was designed specifically to quantify the impact of nonuniform distributions of radioactivity in tissues on the biologic effect of the incorporated radionuclides (*26*,*28*). This model provides a high degree of control over the percentage of radiolabeled cells in the cluster and therefore makes an excellent model to examine the effects of nonuniform distributions of ^{131}I.

To assess the effects of nonuniform distributions of ^{131}I, multicellular clusters were prepared by assembling clusters with mixtures of unlabeled cells and cells radiolabeled with ^{131}IdU. This radiochemical, a thymidine analog, is incorporated into the DNA in the cell nucleus. It was chosen for its capacity to remain within the cell nucleus without migrating to neighboring unlabeled cells (*26*). The survival curves in Figure 3 correspond to the cases where 100%, 10%, or 1%

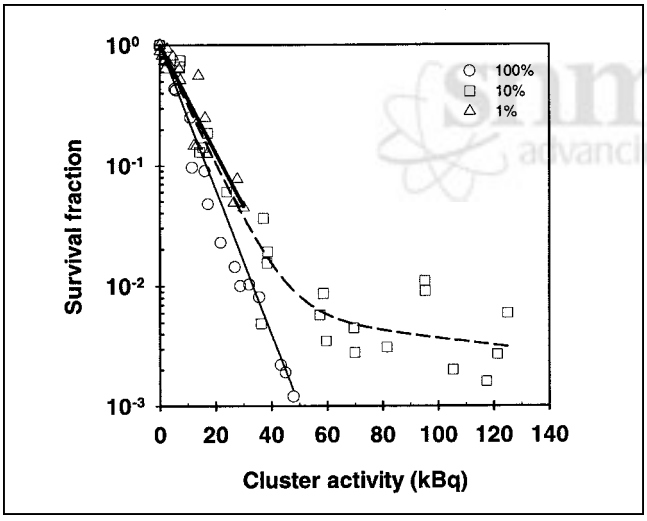

FIGURE 4. Survival of V79 cells in multicellular clusters as function of initial ^{131}I activity per cluster. Data are shown for experiments where 100% (○), 10% (□), or 1% (△) of cells in multicellular cluster were labeled with ^{131}IdU. Clusters were maintained at 10.5°C for 72 h and then survival fraction was determined compared with that of cells from control clusters (0% labeled). Least-squares fits of data corresponding to each labeling condition are shown: 100% (thin line), 10% (dashed line), 1% (bold line).

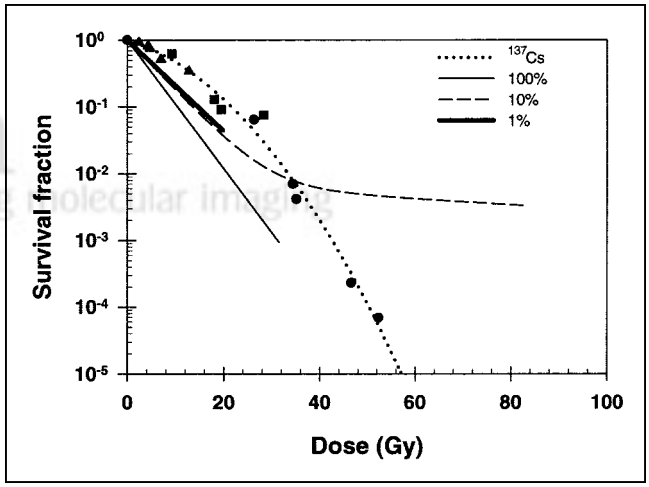

FIGURE 5. Survival of V79 cells after chronic irradiation of multicellular clusters with ^{137}Cs γ-rays. All irradiations were performed at 10.5°C over 72-h period. Data from 3 independent experiments are shown (●, ■, ▲); ▲ represents data reported earlier (*26*). Additional data was acquired to define survival curve at low survival fractions and thereby allow comparison between ^{137}Cs and ^{131}IdU dose–response curves. Dotted curve represents least-squares fit of ^{137}Cs data to linear quadratic model. For comparison, least-squares fits of ^{131}IdU data (survival fraction vs. mean absorbed dose to cluster) to 2-component exponential function are also shown for 3 labeling conditions: 100% (thin line), 10% (dashed line), 1% (bold line).

of the cells was labeled. In all 3 cases, the initial response is exponential with A_1 values of 1.71, 21.7, and 241 mBq per labeled cell, respectively (Table 2). These values are essentially the activity per labeled cell required to achieve 37% survival. As expected, to achieve the same level of overall kill, one has to put substantially more radioactivity per cell as the percentage of labeled cells decreases. Interestingly, while the percentage of labeled cells changes by factors of 10 and 100, the required activity changes by factors of 12.7 and 141. These differences are likely due to the changes in activity distribution in the cluster and perhaps the nature of the radiotoxicity imparted by the radiochemical ^{131}IdU. These points and the tailing of the curve in the case of 10% labeling will be discussed more fully in the context of Figure 4.

Virtually all radioactivity distributions in tissues are nonuniform. At some spatial level, however, the radioactivity distribution may be considered "uniform" depending on the radiation type and energy, tissue geometry, biologic endpoint, and numerous other factors. The multicellular cluster model used in this work allows one to maintain what appears to be a uniform distribution at the macroscopic level (i.e., the labeled cells are randomly distributed in the cluster) while altering the distribution of radioactivity at the multicellular level. By some standards, one may consider this distribution of ^{131}I to be uniform because of its capacity to cross-irradiate cells that reside as much as 30–40 cell diameters distant from the labeled cell. Accordingly, the survival fraction is also plotted as a function of the total activity in the cluster in Figure 4. The mean absorbed dose to the cluster is directly related to the cluster activity. According to the MIRD schema (*33*), the mean absorbed dose to the cluster D is given by:

$$D = \tilde{A}S, \qquad \text{Eq. 2}$$

where $\tilde{A}$ is the cumulated activity and S is the mean absorbed dose per unit cumulated activity. The cumulated activity in the cluster during the 72-h period at 10.5°C is:

$$\tilde{A} = \int_0^{72\,\mathrm{h}} A(t)dt. \qquad \text{Eq. 3}$$

The cluster activity is given by $A(t) = A_o \exp(-0.693t/T_p)$, where A_o is the initial cluster activity and T_p is the physical half-life (8.04 d). Integration of Equation 3 gives $\tilde{A} = 2.28 \times 10^5 A_o$ s. The mean absorbed dose per unit cumulated activity S was calculated using the methods and computer code described by Howell et al. (*12*). From the Materials and Methods, the mass of the cluster of V79 cells is 7.9 ± 0.1 mg. Assuming that the cluster is a 7.9-mg sphere of water containing uniformly distributed ^{131}I, the calculated S value is 2.89×10^{-9} Gy/Bq-s (*12*). This S value takes into account both particulate and photon emissions from ^{131}I. Substitution of $\tilde{A}$ and S into Equation 2 gives D = 0.66 Gy/kBq of cluster activity. The survival fraction versus the mean absorbed dose to the cluster is plotted in Figure 5 for each of the 3 labeling conditions along with the dose–response curve for chronic ^{137}Cs γ-rays. Using the fitted parameters in Table 2, the mean cluster doses required to achieve 37% survival D_{37} for 100%, 10%, and 1% labeling are 4.5, 5.7, and 6.4 Gy, respectively (Table 3). These may be compared with the value of 12.2 Gy obtained for chronic ^{137}Cs γ-rays, thereby suggesting that ^{131}I β-particles may be somewhat more lethal than ^{137}Cs 661.7-keV γ-rays. It is apparent, however, that this conclusion is substantially dependent on the survival fraction at which the comparison is made (Fig. 5).

In addition to the differences in the D_{37} values for chronic ^{137}Cs γ-rays and ^{131}IdU under different labeling conditions, the shapes of the survival curves have marked differences. The dose–response curve for chronic ^{137}Cs γ-rays (Fig. 5) exhibits a shoulder that is typical of the response to low-LET (linear energy transfer) radiations. In contrast, the survival curve for 100% labeling is exponential over 3 logarithms of kill despite the fact that the β-particles emitted by ^{131}I are considered to be similarly low-LET in nature. Although exponential curves are usually associated with responses to high-LET radiations such as α-particles, one must keep in mind that a nonuniform dose distribution can substantially affect the dose–response of a population of cells (*22*,*34*). Even for the case of 100% labeling, all cells in the cluster do not receive the same absorbed dose. It is well known that when β-emitters are uniformly distributed in a sphere, the dose rate at the surface of the sphere is about one half of the dose rate at the center of the sphere (*35*). So even under conditions of a uniform distribution of ^{131}I (i.e., 100% labeling), the dose received by the cells in the cluster varies by a factor of 2. The variations in our cluster model may perhaps be even somewhat larger than this given that the cluster geometry (Fig. 1) is not spherical. These variations may have an impact on the shape of the survival curve. An alternate explanation is that the damage imparted by ^{131}IdU is somewhat like high-LET damage because the decays occur within the DNA. There is evidence to support that the relative biologic effectiveness (RBE) of ^{131}IdU compared with external photons is substantially >1 (*30*,*36*). However, there is also evidence to suggest that the radiotoxicity of ^{131}IdU is of a low-LET nature (*37*–*39*). Therefore, it is not clear at present whether the RBE has any impact on the shape of the survival curve for 100% labeling.

TABLE 3
Mean Lethal Doses for V79 Cells in Multicellular Cluster

Treatment	Cells labeled (%)	D_{37} (Gy)
^{131}IdU	100	4.5 ± 0.2
^{131}IdU	10	5.7 ± 0.7
^{131}IdU	1	6.4 ± 0.5
^{137}Cs γ-rays (chronic)	—	12.2 ± 2.4

Although the data for 100% labeling are indeed interesting, the survival curve observed when 10% of the cells are labeled is perhaps of more importance given that it may better reflect what may occur in vivo. In the case of 10% labeling, there is a distinct tailing of the survival curve at high cluster activities. The tail begins at approximately 1% survival. One possible reason for this is that a small subpopulation of cells (~0.5%–1% of the cells in the cluster) receive a substantially lower dose than the remaining cells. There are several factors that could contribute to this circumstance. The geometry of the cluster is one possibility. As described in the Materials and Methods, the multicellular cluster is formed by gently centrifuging (1,000 rpm) the 4×10^6 cells in a 400-μL microcentrifuge tube. The resulting cluster roughly approximates a sphere; however, on microscopic examination with a dissecting microscope, it may be more accurately described as a paraboloid. Furthermore, the angle of the centrifuge buckets during the pellet formation causes the surface of the top of the paraboloid to be somewhat angled as opposed to flat (increasing centrifugation speed to 2,000 rpm does not change shape). This geometry could result in a relatively low cross-dose being delivered to some of the cells around the top edge of the cluster. However, arguing against this hypothesis are our earlier results for 10% labeling with ^{125}IdU where no tail was observed (*28*). Regardless of the reasons for the tail, it is clear that when 10% of the cells in the cluster are labeled at random, the distribution of radioactivity is uniform from a macroscopic perspective, yet nonuniform from a multicellular level perspective. The nonuniformities at the multicellular level have a significant impact on the biologic response of the population as a whole. Accordingly, dosimetry calculations at the cellular and multicellular levels (*18*), coupled with dose–response modeling at the cellular level, may provide a means to resolve these issues.

The preceding discussion has focused largely on the 100% and 10% labeling cases. For 1% labeling, Figure 4 shows an exponential drop in the survival fraction down to about 5% survival. The slope of the curve is essentially the same as the case for 10% labeling as evidenced by the similar values of A_1 obtained with the curve fits to survival versus cluster activity (Table 2). This suggests that, down to at least 5% survival, the lethal effects imparted to the cell population in the cluster by a given cluster activity are essentially the same for 1% labeling and 10% labeling. It remains to be seen what occurs beyond 5% survival in the 1% labeling case. These effects are notably different from the 100% labeling case. It should be noted that in the 1% and 10% cases, the dose–response curve is largely dictated by the response of the unlabeled cells (receive cross-dose only) because the first 10% of the kill is largely the labeled cell population (receives cross-dose and large self-dose). In contrast, the dose–response curve for the 100% case is entirely for labeled cells. Therefore, the differences in slopes in the dose–response curves suggests that the self-dose to labeled cells is slightly more lethal than the cross-dose to unlabeled cells.

CONCLUSION

Based on our findings with a 3-dimensional multicellular tissue culture model, it may be concluded that when the distribution of ^{131}I is uniform at the macroscopic level, but nonuniform at the multicellular level, the mean absorbed dose to a tissue element may not be a suitable quantity for use in predicting biologic effects in the cell population within the tissue element. Rather, cellular and multicellular dosimetry approaches may be necessary. The MIRD schema is capable of handling such approaches (*7*,*40*). Dose–response modeling using cellular and multicellular dosimetry approaches are currently underway in this laboratory.

The clinical implications of our findings are apparent. However, current nuclear medicine imaging technology (SPECT, PET) cannot provide information regarding distribution of radioactivity at the multicellular level. Such information can only be obtained through detailed analysis of biopsy specimens. Though it is not likely that such detailed analyses can be performed for each patient, it is possible that generalizations regarding the microscopic distribution (i.e., fraction of cells labeled) of a given radiopharmaceutical in tissue can be made based on a limited number of samples. Such information could in turn be used to predict biologic response using cellular and multicellular dosimetry approaches.

ACKNOWLEDGMENTS

The authors thank Tiffany Cooke for assistance in carrying out the experiments during her summer undergraduate internship program. The authors also acknowledge Venkata Lanka and the personnel in the UMDNJ Office of Radiation Safety Services for assisting with determination of absorbed dose delivered by the ^{137}Cs irradiator and synthesis of ^{131}IdU. Many helpful discussions with Drs. Edouard I. Azzam, Sonia M. deToledo, and Bogdan I. Gerashchenko are highly acknowledged. Finally, the use of Dr. John Bogden's analytical balance is also appreciated. This work was supported in part by U.S. Public Health Service grant R01CA83838.

REFERENCES

1. Weber DA, Eckerman KF, Dillman LT, Ryman JC. *MIRD: Radionuclide Data and Decay Schemes.* New York, NY: Society of Nuclear Medicine; 1989:229.
2. ICRU. *Stopping Powers for Electrons and Positrons*. Report 37. Bethesda, MD: International Commission on Radiation Units and Measurements; 1984:206.
3. Hamilton JG. The use of radioactive tracers in biology and medicine. *Radiology*. 1942;39:541–572.
4. Sinclair WK, Abbatt JD, Farran HE, Harriss EB, Lamerton LF. A quantitative autoradiographic study of radioiodine distribution and dosage in human thyroid glands. *Br J Radiol.* 1956;29:36–41.
5. Loevinger R, Holt JG, Hine GJ. Internally administered radioisotopes. In: Hine GJ, Brownell GL, eds. *Radiation Dosimetry*. New York, NY: Academic Press; 1956:801–873.
6. Adelstein SJ. Heterogeneity of dose-distribution in nuclear medicine. In: Poznan-

ski AK, ed. *Radiation Protection in Medicine.* Bethesda, MD: National Council on Radiation Protection and Measurements; 1993:122–131.
7. ICRU. ICRU Report No. 67: Absorbed-dose specification in nuclear medicine. *J ICRU.* 2002;2:3–110.
8. Rossi HH, Ellis RH. Calculations for distributed sources of beta radiation. *AJR.* 1952;67:980–988.
9. Tisljar-Lentulis G, Feinendegen LE, Walther H. Calculation of specific energies of incorporated Pu-239 and I-131 in accordance with the concept of the critical cell. *Radiat Environ Biophys.* 1976;13:197–204.
10. Roesch WC. Microdosimetry of internal sources. *Radiat Res.* 1977;70:494–510.
11. Kwok CS, Prestwich WV, Wilson BC. Calculation of radiation doses for nonuniformly distributed beta and gamma radionuclides in soft tissue. *Med Phys.* 1985;12:405–412.
12. Howell RW, Rao DV, Sastry KSR. Macroscopic dosimetry for radioimmunotherapy: nonuniform activity distributions in solid tumors. *Med Phys.* 1989;16: 66–74.
13. Wheldon TE, O'Donoghue JA. The radiobiology of targeted radiotherapy. *Int J Radiat Biol.* 1990;58:1–21.
14. Hui TE, Fisher DR, Press OW, et al. Localized beta dosimetry of ^{131}I-labeled antibodies in follicular lymphoma. *Med Phys.* 1992;19:97–104.
15. Humm JL, Cobb LM. Nonuniformity of tumor dose in radioimmunotherapy. *J Nucl Med.* 1990;31:75–83.
16. Fisher DR. From "micro" to "macro" internal dosimetry. In: Raabe O, ed. *Internal Radiation Dosimetry: Health Physics Society 1994 Summer School.* Madison, WI: Medical Physics Publishing; 1994:61–80.
17. Bolch WE, Bouchet LG, Robertson JS, et al. MIRD Pamphlet No. 17: The dosimetry of nonuniform activity distributions—radionuclide S values at the voxel level. *J Nucl Med.* 1999;40(suppl):11S–36S.
18. Goddu SM, Rao DV, Howell RW. Multicellular dosimetry for micrometastases: dependence of self-dose versus cross-dose to cell nuclei on type and energy of radiation and subcellular distribution of radionuclides. *J Nucl Med.* 1994;35:521–530.
19. Roberson PL, Buchsbaum DJ, Heidorn DB, Ten Haken RK. Three-dimensional tumor dosimetry for radioimmunotherapy using serial autoradiography. *Int J Radiat Oncol Biol Phys.* 1992;24:329–334.
20. Yorke ED, Williams LE, Demidecki AJ, Heidorn DB, Roberson PL, Wessels BW. Multicellular dosimetry for beta-emitting radionuclides: autoradiography, thermoluminescent dosimetry and three-dimensional dose calculations. *Med Phys.* 1993;20(part 2):543–550.
21. Humm JL, Macklis RM, Bump K, Cobb LM, Chin LM. Internal dosimetry using data derived from autoradiographs. *J Nucl Med.* 1993;34:1811–1817.
22. O'Donoghue JA. Implications of nonuniform tumor doses for radioimmunotherapy. *J Nucl Med.* 1999;40:1337–1341.
23. Kwok CS, Crivici A, MacGregor WD, Unger MW. Optimization of radioimmunotherapy using human malignant melanoma multicell spheroids as a model. *Cancer Res.* 1989;49:3276–3281.
24. Langmuir VK, McGann JK, Buchegger F, Sutherland RM. ^{131}I-Anticarcinoembryonic antigen therapy of LS174T human colon adenocarcinoma spheroids. *Cancer Res.* 1989;49:3401–3406.
25. Harapanhalli RS, Narra VR, Yaghmai V, et al. Vitamins as radioprotectors in vivo. II. Protection by vitamin A and soybean oil against radiation damage caused by internal radionuclides. *Radiat Res.* 1994;139:115–122.
26. Bishayee A, Rao DV, Howell RW. Evidence for pronounced bystander effects caused by nonuniform distributions of radioactivity using a novel three-dimensional tissue culture model. *Radiat Res.* 1999;152:88–97.
27. Bishayee A, Hill HZ, Stein D, Rao DV, Howell RW. Free-radical initiated and gap junction-mediated bystander effect due to nonuniform distribution of incorporated radioactivity in a three-dimensional tissue culture model. *Radiat Res.* 2001;155:335–344.
28. Howell RW, Bishayee A. Bystander effects caused by nonuniform distributions of DNA-incorporated ^{125}I. *Micron.* 2002;33:127–132.
29. Howell RW, Goddu SM, Bishayee A, Rao DV. Radioprotection against lethal damage caused by chronic irradiation with radionuclides in vitro. *Radiat Res.* 1998;150:391–399.
30. Bishayee A, Rao DV, Bouchet LG, Bolch WE, Howell RW. Radioprotection by DMSO against cell death caused by intracellularly localized I-125, I-131, and Po-210. *Radiat Res.* 2000;153:416–427.
31. ICRP. *Recommendations of the International Commission on Radiological Protection.* Publication 60. Oxford, U.K.: Pergamon Press; 1990:79–89.
32. Makrigiorgos GM, Adelstein SJ, Kassis AI. Cellular radiation dosimetry and its implications for estimation of radiation risks: illustrative results with technetium-99m-labeled microspheres and macroaggregates. *JAMA.* 1990;264:592–595.
33. Loevinger R, Budinger TF, Watson EE. *MIRD Primer for Absorbed Dose Calculations.* Revised. New York, NY: The Society of Nuclear Medicine; 1991:9.
34. Humm JL, Chin LM. A model of cell inactivation by alpha-particle internal emitters. *Radiat Res.* 1993;134:143–150.
35. Loevinger R, Japha EM, Brownell GL. Discrete radioisotope sources. In: Hine GJ, Brownell GL, eds. *Radiation Dosimetry.* New York, NY: Academic Press; 1956:693–755.
36. Whaley JM, Little JB. Efficient mutation induction by I-125 and I-131 decays in DNA of human cells. *Radiat Res.* 1990;123:68–74.
37. Hofer KG, Hughes WL. Radiotoxicity of intranuclear tritium, iodine-125 and iodine-131. *Radiat Res.* 1971;47:94–109.
38. Chan PC, Lisco E, Lisco H, Adelstein SJ. The radiotoxicity of iodine-125 in mammalian cells: a comparative study on cell survival and cytogenic responses to ^{125}IUdR, ^{131}IUdR, and ^{3}HTdR. *Radiat Res.* 1976;67:332–343.
39. Narra VR, Howell RW, Harapanhalli RS, Sastry KSR, Rao DV. Radiotoxicity of some I-123, I-125, and I-131 labeled compounds in mouse testes: implications for radiopharmaceutical design. *J Nucl Med.* 1992;33:2196–2201.
40. Howell RW, Wessels BW, Loevinger R. The MIRD perspective 1999. *J Nucl Med.* 1999;40(suppl):3S–10S.